suppresses the Jahn-Teller distortion and eliminates, to a large degree, the Franck-Condon reduction of the bandwidth.

Experimental consequences. (i) Because pair-binding does not occur for two and four added electrons, we expect that materials such as K_2C_{60} or K_4C_{60} would not superconduct (*21*). (ii) The superconducting transition temperature, T_c, should peak when there are approximately an odd number of electrons per molecule. Of course, some of the long-distance physics not included in this calculation may favor a particular concentration of dopants in the solid (*22*). (iii) With the help of different dopants it is possible to drive the system ferromagnetic. In fact, there is also a narrow range of U, between U_{FM} and U_{pair}, in which the singlet state is favored over the triplet state, and hence in principle it is possible to drive the system antiferromagnetic as well. (iv) The pressure dependences of T_c discussed above should be noted. For the case in which $W_i > E_{pair}$ we predict an approximately linear dependence of ln T_c on the intermolecular bandwidth (*23*). (v) Because for large enough U, the doubly charged C_{60} should be in an orbital singlet state, the infrared absorption should be quite different from what one would expect from the single particle theory (*19*).

REFERENCES AND NOTES

1. H. W. Kroto *et al.*, *Nature* **318**, 162 (1985); W. Kratschmer *et al.*, *ibid.* **347**, 354 (1990); H. Ajie *et al.*, *J. Phys. Chem.* **94**, 8630 (1990).
2. A. F. Hebard *et al.*, *Nature* **350**, 600 (1991); M. J. Rosseinsky *et al.*, *Phys. Rev. Lett.* **66**, 2830 (1991).
3. K. Holczer *et al.*, *Science* **252**, 1154 (1991); K. Holczer *et al.*, *Phys. Rev. Lett.* **67**, 271 (1991).
4. P.-M. Allemand *et al.*, *Science* **253**, 301 (1991).
5. S. Chakravarty and S. Kivelson, *Europhys. Lett.*, in press.
6. A. J. Heeger *et al.*, *Rev. Mod. Phys.* **60**, 781 (1988).
7. V. Elser and R. C. Haddon, *Nature* **325**, 792 (1987).
8. R. C. Haddon, L. E. Brus, K. Raghavachari, *Chem. Phys. Lett.* **125**, 459 (1986).
9. L. Pauling, *Proc. R. Soc. London Ser. A* **196**, 343 (1949).
10. P. W. Anderson, *Mater. Res. Bull.* **8**, 153 (1973); *Science* **235**, 1196 (1987); in *High Temperature Superconductivity: Proceedings*, K. S. Bedell *et al.*, Eds. (Addison-Wesley, Reading, MA, 1990).
11. S. A. Kivelson, D. S. Rokhshar, J. Sethna, *Phys. Rev. B* **35**, 8865 (1987).
12. G. Baskaran and E. Tossatti, *Curr. Sci.* **61**, 33 (1991).
13. L. Landau and E. M. Lifshitz, *Quantum Mechanics* (Pergamon, New York, ed. 3, 1977), vol. 3.
14. If we define $\epsilon(n) = -100.80069 + 0.321666n$. Then for $t'/t = 1.2$: $\Phi_0(L = 0, S = 0) = \epsilon(0) + 15(U/t) - 0.74785(U/t)^2$, $\Phi_1(L = 1, S = 1/2) = \epsilon(1) + 15.5(U/t) - 0.73772(U/t)^2$, $\Phi_2(L = 1, S = 1) = \epsilon(2) + 16(U/t) - 0.72557(U/t)^2$, $\Phi_2(L = 0, S = 0) = \epsilon(2) + 16.05(U/t) - 0.74237(U/t)^2$, $\Phi_2(L = 2, S = 0) = \epsilon(2) + 16.02(U/t) - 0.73128(U/t)^2$, $\Phi_3(L = 0, S = 3/2) = \epsilon(3) + 16.5(U/t) - 0.71140(U/t)^2$, $\Phi_3(L = 1, S = 1/2) = \epsilon(3) + 16.55(U/t) - 0.72725(U/t)^2$, $\Phi_3(L = 2, S = 1/2) = \epsilon(3) + 16.53(U/t) - 0.71991(U/t)^2$, $\Phi_4(L = 1, S = 1) = \epsilon(4) + 17.05(U/t) - 0.71012(U/t)^2$, $\Phi_4(L = 0, S = 0) = \epsilon(4) + 17.10(U/t) - 0.72671(U/t)^2$, $\Phi_4(L = 2, S = 0) = \epsilon(4) + 17.07(U/t) - 0.71575(U/t)^2$, $\Phi_5(L = 1, S = 1/2) = \epsilon(5) + 17.6(U/t) - 0.70661(U/t)^2$, and $\Phi_6(L = 0, S = 0) = \epsilon(6) + 18.15(U/t) - 0.70087(U/t)^2$. All energies are in units of t. We have explored the range $1.0 \leq t'/t \leq 1.35$ and have found that the basic picture described in the text is the same over the entire range.
15. S. R. White, S. Chakravarty, M. P. Gelfand, S. Kivelson, in preparation.
16. P. W. Stephens *et al.*, *Nature* **351**, 632 (1991).
17. Y. Nagaoka, *Prog. Theor. Phys.* **52**, 1716 (1974). Although Nagaoka discusses the degeneracy of charge density wave and superconducting orders for bipartite lattices, the extension to a frustrated FCC lattice is trivial. In this case the superconducting state has considerably lower energy than the charge density wave state.
18. R. P. Feynman, R. B. Leighton, M. Sands, *The Feynman Lectures on Physics* (Addison-Wesley, Reading, 1964), vol. 3, see especially sec. 15-5.
19. M. Salkola, S. Chakravarty, S. Kivelson, in preparation.
20. P. W. Anderson, *Phys. Rev. Lett.* **34**, 953 (1975).
21. Indeed, recent experiments have shown that A_4C_{60} does not superconduct, where A is K, Rb, or mixtures of K, Rb, or Cs. See R. M. Fleming *et al.*, *Nature* **352**, 701 (1991).
22. The structure of K_3C_{60} is now known to be fcc (*16*), where both the octahedral and the tetrahedral sites are occupied by the K^+ ions, with a lattice constant that is virtually unchanged from the pure C_{60} solid. It is therefore reasonable to assume that doping fills the lowest unoccupied states of the molecule, while leaving the electronic structure of a single molecule essentially unchanged, in particular, the threefold degeneracy of the highest unoccupied orbitals. Any other composition is likely to produce significant distortions in the solid.
23. G. Sparn *et al.*, *Science* **252**, 1829 (1991); G. Sparn *et al.*, in preparation.

24. It is a great pleasure to thank P. W. Anderson for his comments and K. Holczer for numerous exciting discussions of the rapidly developing experimental scene. In particular, we would like to thank P. W. Anderson for drawing our attention to the fact that the symmetry-preserving intramolecular phonons are pair enhancing whereas the symmetry breaking phonons are pair breaking. We thank S. R. White and M. Salkola for collaborations to be reported elsewhere (*15, 19*). Thanks are also due to E. Abrahams, A. Auerbach, V. Emery, I. Pimentel, D. Rokhsar, and P. Scharf for particularly helpful discussions. Supported by the National Science Foundation grants no. DMR-89-07664 (S.C.) and no. DMR-90-11803 (S.K.).

22 September 1991; accepted 10 October 1991

Protein Hydration in Aqueous Solution

GOTTFRIED OTTING, EDVARDS LIEPINSH, KURT WÜTHRICH

High-resolution proton nuclear magnetic resonance studies of protein hydration in aqueous solution show that there are two qualitatively different types of hydration sites. A well-defined, small number of water molecules in the interior of the protein are in identical locations in the crystal structure and in solution, and their residence times are in the range from about 10^{-2} to 10^{-8} second. Hydration of the protein surface in solution is by water molecules with residence times in the subnanosecond range, even when they are located in hydration sites that contain well-ordered water in the x-ray structures of protein single crystals.

PROTEIN FOLDING, THAT IS, THE RELATIONS BETWEEN AMINO acid sequence, folding pathways, and kinetics, and the functional spatial arrangement of a polypeptide chain, is presently the least well understood step in a "central dogma" relating storage of genetic information with its expression by protein functions (*1*). New insights can be anticipated from structural characterization of both the unfolded and the functional folded polypeptide chain under the conditions of the folding milieu. Because water is excluded almost entirely from the interior of globular proteins (*1, 2*), different solvation of the polypeptide chain in the unfolded and folded forms must be an important factor. This article reports on investigations of the hydration of two polypeptides in aqueous solution. The hormone oxytocin has been chosen as a model for the

The authors are in the Institut für Molekularbiologie und Biophysik, Eidgenössische Technische Hochschule–Hönggerberg, CH-8093 Zürich, Switzerland.

highly solvated, unfolded state, since most atoms in this nonapeptide are solvent exposed in a predominantly flexible, nonglobular solution conformation (*3*). Bovine pancreatic trypsin inhibitor (BPTI) has been selected to represent globular proteins. For both molecules, high-resolution crystal structures are available that also include a range of hydration water molecules (*4–7*).

There are two classes of experiments capable of providing structural information at atomic resolution on protein molecules. One consists of x-ray diffraction and neutron diffraction studies with protein crystals (*8*). The coordinates of the oxygen atoms of numerous hydration water molecules are usually included in the description of a high-resolution protein crystal structure, suggesting that at least part of the hydration shell is well defined (*9*). Overall, the protein crystal structures deposited to date in the Brookhaven Protein Data Bank (*10*) include the coordinates of over 30,000 water oxygen atoms. The second experimental approach is nuclear magnetic resonance (NMR) spectroscopy with protein solutions (*11, 12*). Although the NMR method for protein structure determination has been available since 1985 (*13*), hydration water molecules proved to be evasive to detection in aqueous solution, and the observation of individual water molecules in a globular protein was reported only in 1989 (*14*). In the present study we used new NMR experiments (*15*) that enable studies of both the location and the residence time of individual hydration water molecules on the surface of flexible polypeptide chains or globular proteins in aqueous solution. Results obtained with this novel approach are presented and evaluated relative to the corresponding crystal structure data.

NMR and protein hydration. NMR experiments for studies of protein hydration rely primarily on phenomena related to nuclear spin relaxation (*16*). Beginning in the 1970's, measurements of relaxation dispersion in the bulk water signal of protein solutions have provided evidence that at least part of the water associated with proteins is highly mobile, with residence times in the hydration sites in the subnanosecond range [see, for example, (*17, 18*)]. In early one-dimensional (1D) high-resolution ^{1}H NMR experiments performed with selective water irradiation, nuclear Overhauser effects (NOE) between water protons and polypeptide protons were observed, but no further information on the kinetic stability of the hydration sites was obtained (*19*). Individual water molecules bound to hydration sites in a globular protein in solution were eventually observed with the use of 2D NOE spectroscopy (NOESY) (*14*) and heteronuclear 3D experiments (*20, 21*). However, in BPTI only four water molecules located in the interior of the protein were detected, and no NOEs were seen that would correspond to close contacts of protein protons with the surface hydration waters observed by x-ray diffraction in BPTI crystals (*5–7*). These observations were confirmed by NMR studies of interleukin-1β in aqueous solution, where similar NMR experiments detected exclusively hydration water molecules in the interior of the protein in identical locations as in the crystal structure (*21*).

The previous apparent absence of NOEs with water molecules in surface hydration sites is a consequence of the technical difficulties of the NMR experiments used. In all of the studies performed to date, the protein-bound hydration water molecules, including waters located in the interior, were found to exchange rapidly on the time scale of chemical shift differences, that is, with residence times in the hydration sites in the millisecond range or shorter (*22*). Therefore only a single signal is observed for the protons of the hydration water and the bulk water. For the same reason, the ^{1}H NMR lines of all -COOH groups, αNH_3^+, and most -OH groups of the polypeptide chain usually coincide with the bulk water resonance. As a consequence, NOEs can be assigned to different hydration water molecules only by reference to the individually assigned polypeptide ^{1}H NMR lines of the 3D protein structure (*14*). Furthermore, in 2D experiments the NOEs with the protons at the bulk water chemical shift are all located on the same 1D cross section, which is then quite crowded with lines. In the present study we obtained improved resolution with homonuclear 3D NMR experiments, and novel solvent suppression schemes were used for the suppression of the dominant bulk water signal after the NOE transfer of magnetization from the hydration waters to the protons of the polypeptide. These NMR technical details have been described in detail elsewhere (*15, 23*).

In the systems of interest here, ^{1}H spin relaxation and NOEs are dominated by time-dependent dipole-dipole coupling between nearby protons (*16*). In the simplest model the hydrated protein is represented by a rigid sphere (Fig. 1A). The intensity of the NOE between two hydrogen atoms i and j is then proportional to d_{ij}^{-6}, where d_{ij} is the distance between the two protons (Fig. 1A). It is further related to a correlation function describing the stochastic motions of the vector $\mathbf{d}_{ij}$ that connects the two protons. The strong distance dependence implies that NOEs can be observed only between spatially close protons, that is, in practice for $d_{ij} \lesssim 4.0$ Å. In the rigid model of Fig. 1A one would expect to observe more than 200 NOEs between protons of BPTI and the ~60 hydration waters reported in the crystal structures of this protein (*5–7*). However, these NOEs could be quenched by additional rapid motions of the water molecules relative to the protein surface, which would explain why they were not detected in the earlier studies (*14, 20, 21*).

The NOEs can be measured either by experiments in the laboratory frame of reference (NOESY) or in the rotating frame (ROESY) (*24*). If sufficiently short mixing times are used to minimize contributions from autorelaxation and spin diffusion (*11, 25*), the measured NOE intensities reflect directly the cross relaxation rates in the laboratory frame, σ^{NOE}, or in the rotating frame, σ^{ROE}, respectively. The two rates differ in their functional dependence on the spectral densities, $J(\omega)$ (*24*):

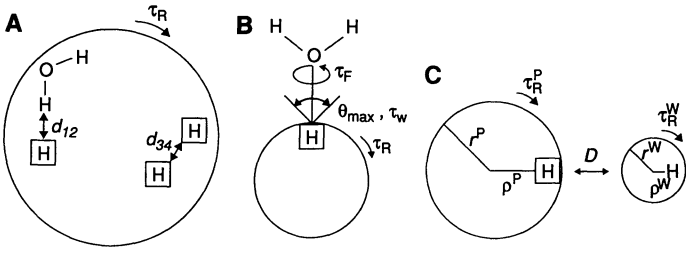

Fig. 1. Three models used in this article to calculate dipole-dipole cross relaxation rates σ^{NOE} and σ^{ROE}. (**A**) Isotropic rotational diffusion of a rigid sphere. Water molecules in the first hydration shell are considered to be part of the sphere representing the protein. Squares represent polypeptide protons. The vector d_{12} connects a polypeptide proton with a hydration water proton, and d_{34} connects two polypeptide protons. τ_R is the correlation time for the overall rotation of the sphere, which is in this model equal to the effective correlation time for the modulation of the dipolar interactions. (**B**) Wobbling in a cone model (*26, 27*). The residence time of the water molecules in the hydration sites is assumed to be long compared to the rotational correlation time τ_R, but the water rotates with a correlation time τ_F around a hydrogen bond to the protein, and this rotation axis is free to wobble with a correlation time τ_w within a cone with an opening angle $\theta_{max} = \pm 45°$. The overall rotational tumbling of the hydrated protein is again described by an equivalent sphere, with a correlation time τ_R. (**C**) Random, independent translation and rotation of the protein and the water molecule. The two molecules are represented by spheres of radius r^P and r^W, respectively, with the proton spin displaced from the center by ρ^P and ρ^W. The translational diffusion coefficient D characterizes the relative translational motions of the two molecules. The two spheres reorientate isotropically with correlation times τ_R^P and τ_R^W, respectively.

$$\sigma^{NOE} = 6J(2\omega_0) - J(0) \quad (1)$$

$$\sigma^{ROE} = 3J(\omega_0) + 2J(0) \quad (2)$$

where ω_0 is the Larmor frequency of the protons. Equations 1 and 2 show that σ^{ROE} is always positive because the spectral densities $J(\omega)$ have finite positive values at all frequencies (*16*). In contrast, the sign of σ^{NOE} depends on the explicit functional form of $J(2\omega_0)$ and $J(0)$, which in turn is related to the rate processes that govern the modulation of the dipole-dipole coupling. In the following section we investigate how sign and value of the ratio $\sigma^{NOE}/\sigma^{ROE}$ can be rationalized by different model representations of a hydrated protein.

Model representations of hydrated proteins. An important conclusion results from the simple model of Fig. 1A. In this rigid, spherical molecule the mobility of the vectors d_{ij} is governed by the overall rotational correlation time, τ_R, independent of whether these vectors connect different polypeptide protons or polypeptide protons with water protons (Fig. 1A). The results of computing σ^{NOE} and σ^{ROE} with the parameters given in the caption to Fig. 2 are displayed in Fig. 2A; $\sigma^{ROE} \geq \sigma^{NOE}$ over the entire range of τ_R values, and σ^{NOE} changes sign at $\omega_0\tau_R \approx 1.12$, corresponding to $\tau_R \approx 300$ ps at a Larmor frequency of 600 MHz. Under the experimental conditions used here (see captions to Figs. 3 and 4), measurements of ^{13}C relaxation times for α-carbon positions showed that the overall rotational tumbling of oxytocin can be characterized by a rotational correlation time for an equivalent sphere of $\tau_R \approx 2$ ns, and for BPTI $\tau_R \approx 8$ ns was extrapolated from earlier measurements at higher temperature (*26*). Correspondingly, for both molecules negative σ^{NOE} values were observed for all NOEs between different polypeptide protons. On the other hand, positive σ^{NOE} rates were detected for numerous intermolecular NOEs with water protons, showing that the polypeptide proton-water proton dipolar interactions must be modulated by additional, higher frequency rate processes.

The "wobbling in a cone" model (*26, 27*) assumes that the hydration water molecules are flexibly bound to a particular hydration site of the protein and have a long residence time compared to the effective rotational correlation time of the protein. Local motions of a water molecule in its hydration site are simulated by a combination of rotation about the hydrogen-bond axis (τ_F) and wobbling motions of this rotation axis inside a cone (τ_W). This model would not predict positive $\sigma^{NOE}/\sigma^{ROE}$ ratios for the protein proton–water proton NOE for any combination of τ_W and τ_F values (Fig. 2B). From studies with this and similar models we had to conclude that the observed positive values for $\sigma^{NOE}/\sigma^{ROE}$ cannot be rationalized by a description of the hydrated protein where the lifetime of the water protons in the hydration sites is long compared to τ_R.

Positive σ^{NOE} values were obtained with the assumption of short residence times of the hydration water, characterized by diffusion coefficients D greater than 3×10^{-6} cm^2/s in the model of Fig. 1C (*28*). [Note that the self-diffusion coefficient of pure water at 6°C is about 12×10^{-6} cm^2/s (*29*)]. The diffusion coefficients can be translated into residence times of the hydration water molecules using the Einstein-Smoluchowski relation

$$\tau = \overline{x^2}/D \quad (3)$$

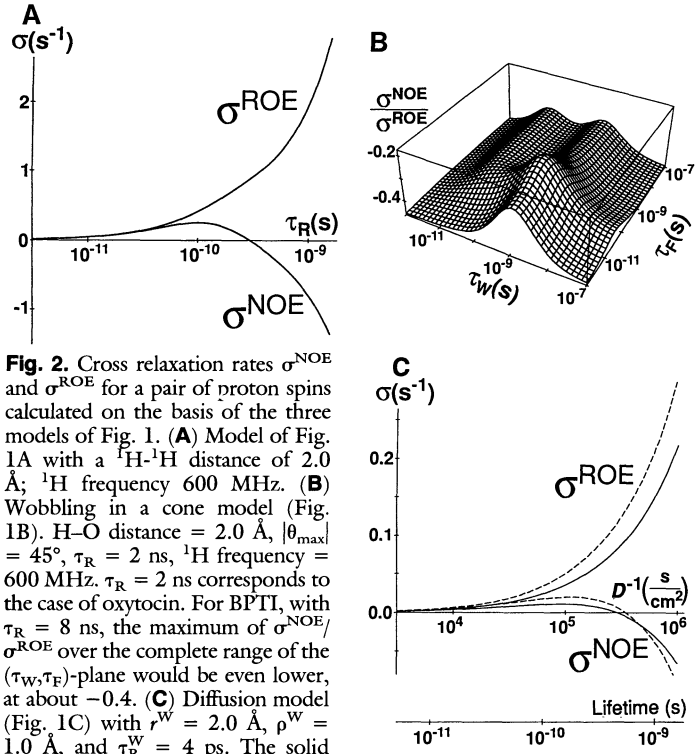

Fig. 2. Cross relaxation rates σ^{NOE} and σ^{ROE} for a pair of proton spins calculated on the basis of the three models of Fig. 1. (**A**) Model of Fig. 1A with a ^1H-^1H distance of 2.0 Å; ^1H frequency 600 MHz. (**B**) Wobbling in a cone model (Fig. 1B). H–O distance = 2.0 Å, $|\theta_{max}|$ = 45°, τ_R = 2 ns, ^1H frequency = 600 MHz. τ_R = 2 ns corresponds to the case of oxytocin. For BPTI, with τ_R = 8 ns, the maximum of $\sigma^{NOE}/\sigma^{ROE}$ over the complete range of the (τ_W,τ_F)-plane would be even lower, at about −0.4. (**C**) Diffusion model (Fig. 1C) with r^W = 2.0 Å, ρ^W = 1.0 Å, and τ_R^W = 4 ps. The solid curve was calculated with r^P = 12.0 Å, ρ^P = 11.0 Å, ^1H frequency = 500 MHz, and τ_R^P = 8 ns to simulate the intermolecular water proton–protein ^1H cross relaxation in the experiment with BPTI at 4°C (Fig. 4). The dashed curve was calculated with r^P = 4.0 Å, ρ^P = 3.0 Å, ^1H frequency = 600 MHz, and τ_R = 2 ns to approximate the situation for the oxytocin experiment at 6°C (Fig. 3). At the bottom the inverse of the translational diffusion coefficient, $1/D$, was converted into the corresponding lifetimes of the hydration water molecules with the Einstein-Smoluchowski relation (see text).

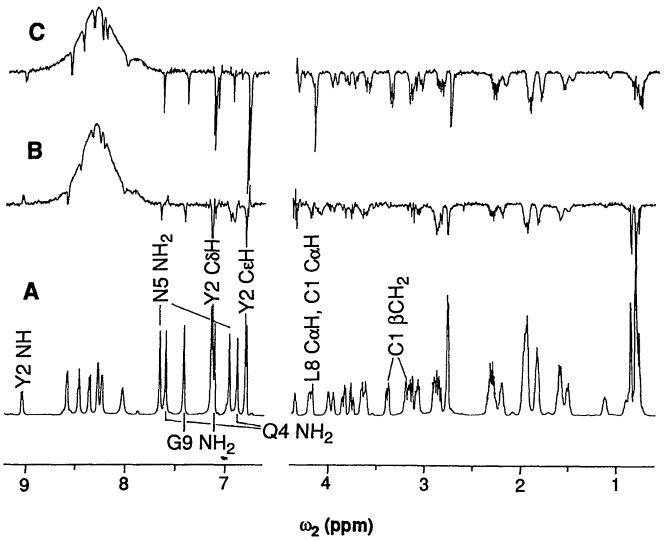

Fig. 3. Proton NMR spectra showing NOEs between oxytocin protons and water protons (oxytocin concentration 50 mM, solvent 90 percent H_2O–10 percent D_2O, T = 6°C, pH = 3.5, ^1H frequency = 600 MHz, experimental schemes of Fig. 1, A and B, in (*15*) with mixing time τ_m = 30 ms, spin locks $SL_{\phi4}$ = 0.5 ms and $SL_{\phi3}$ = $SL_{\phi5}$ = 2 ms, and delay τ = 167 μs). All of the spectra were multiplied with the spectral excitation profile $\sin[0.63(\delta - 4.9)]$, where δ is the chemical shift in ppm, which has excitation maxima at 2.45 and 7.35 ppm. The low-field region from 7 to 9 ppm was inverted for improved readability. (**A**) 1D spectrum. (**B**) Cross section through the NOESY spectrum along ω_2 at the ω_1 frequency of the water line (t_{1max} = 40 ms, t_{2max} = 328 ms, time domain data size 430 × 4096 points, and 32 scans per free induction decay); homospoil pulses of 0.5-ms duration were applied every 2 ms during the first 20 ms of the mixing time to prevent the decay of the water signal by radiation damping). The CεH multiplet fine structure of Tyr[2] is distorted by an artifact that was absent in similar spectra recorded with our AM500 spectrometer. (**C**) Cross section through the ROESY spectrum along ω_2 at the ω_1 frequency of the water line [processed and plotted with identical parameters as in (B)]. Resonance assignments for selected peaks are indicated with the one-letter amino acid symbol and the sequence position (*39*).

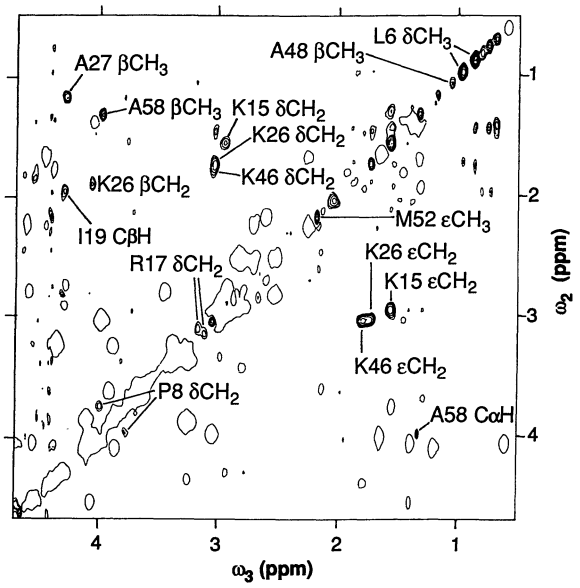

Fig. 4. ω_2-ω_3 cross plane through a homonuclear 3D ^{1}H NOESY-TOCSY spectrum taken at the ω_1 frequency of the water signal and showing NOE cross peaks between protons of BPTI and water protons [BPTI concentration = 20 mM, solvent 90 percent H_2O–10 percent D_2O, T = 4°C, pH = 3.5, ^{1}H frequency = 500 MHz, experimental scheme of Fig. 1C in (*15*), mixing time τ_m = 50 ms, and other parameters as in (*15*)]. For positive peaks only the lowest contour level is plotted. Selected negative peaks (corresponding to $\sigma^{NOE} > 0$) are identified by the assignment of the polypeptide proton that interacts with the water.

If we define an average displacement $(\overline{x^2})^{1/2}$ of 4.0 Å as the criterion for complete water proton exchange in and out of a hydration site, σ^{NOE} is positive for lifetimes shorter than ~500 ps (Fig. 2C). This is much shorter than the lifetime of a proton in a water molecule with respect to exchange by hydrolysis (*30*). We therefore conclude that the observation of positive σ^{NOE} rates indicates rapid exchange of complete water molecules between the bulk solvent and the protein hydration sites.

The NOE cross peaks resulting from positive σ^{NOE} should be small (Fig. 2C). This was confirmed by the NMR experiments (Figs. 3 and 4). At long mixing times, cross peaks arising from positive σ^{NOE} values may be canceled by spin-diffusion from cross peaks with negative σ^{NOE} rates, which are usually more intense.

NMR observations with oxytocin and BPTI. In Fig. 3 are shown the normal 1D ^{1}H NMR spectrum (Fig. 3A) of oxytocin and the cross sections through the 2D NOESY (Fig. 3B) and ROESY (Fig. 3C) spectra, which contain the water-polypeptide cross peaks. With few exceptions which are due to dominant effects from chemical exchange (*31*), the oxytocin signals show negative NOESY cross peaks with the water line, corresponding to positive σ^{NOE} values. In contrast, all intramolecular NOESY cross peaks between different protons of oxytocin were positive, as expected for a molecule in the slow tumbling regime of Fig. 2A (*32*). The rapid exchange of the hydration water molecules implicated by the different sign of intramolecular and intermolecular σ^{NOE} values is further substantiated by a comparison of Fig. 3, B and C, which shows that with few exceptions (*33*) the water-polypeptide cross peaks are two to three times less intense in NOESY than in ROESY. In the model of Fig. 1C this ratio corresponds to lifetimes of the water molecules in the hydration sites of 100 to 250 ps. Virtually all of the ^{1}H NMR lines in Fig. 3A are represented by NOEs in Fig. 3, B and C, showing that all parts of the oxytocin molecule are exposed to the solvent. However, no stably bound water molecules could be identified.

In contrast to oxytocin, the 1D cross section through the water resonance of a 2D ^{1}H NOESY spectrum of BPTI contains numerous overlapping groups of peaks (*14*). They can be virtually completely resolved in homonuclear 3D NOESY-TOCSY (TOCSY, total correlation spectroscopy) and 3D ROESY-TOCSY spectra (*15*). The high-field region from the 2D ω_2-ω_3 cross section taken at the ω_1 frequency of the water resonance in the 3D NOESY-TOCSY spectrum is shown in Fig. 4. The peaks on the diagonal come from the transfer of magnetization from the water line to the protein resonances during the NOESY mixing time. The fact that the ω_2 frequency equals the ω_3 frequency indicates that for these peaks there was no further magnetization transfer during the TOCSY mixing period (*34*). The off-diagonal peaks arise because magnetization precessing during t_2 is transferred to scalar-coupled protons during the TOCSY mixing period; they support the assignment of the diagonal NOE peaks (*15*). The previously reported cross peaks with the interior water molecules and some labile polypeptide protons (*14*) were again observed in these 3D NMR spectra, and many additional NOEs with the water signal could be assigned due to the presence of the off-diagonal peaks. Many of these newly found NOEs have positive σ^{NOE} values and come from solvent-accessible protons on the protein surface. They are much weaker than the positive NOE cross peaks with the interior water molecules, which correspond to negative σ^{NOE} rates (*14*). Except for the cross peaks with the interior waters, the $\sigma^{NOE}/\sigma^{ROE}$ ratios for the observed water-protein interactions are mostly in the range from 0.3 to 0.1. In the model of Fig. 1C these values indicate residence lifetimes in the range from 100 to 300 ps. Based on the experience with oxytocin, one might expect that most or all surface waters of BPTI should show positive σ^{NOE} rates with the water. We attribute the apparent absence of many of the expected peaks to the lower sensitivity (oxytocin was studied at higher concentration and has sharper lines than BPTI) because most of the negative cross peaks seen in Fig. 4 are with intense resonances of BPTI, such as those of methyl groups, or methylene groups with degenerate chemical shifts. This sensitivity criterion applies, however, only to weak NOEs with positive σ^{NOE} values from short-lived hydration waters. Long-lived surface hydration waters would produce much stronger NOEs with negative σ^{NOE} values, comparable to those seen for the internal waters. It is therefore very unlikely that NOEs with surface hydration water molecules bound with residence times >500 ps would have escaped detection by both NOESY and ROESY (Fig. 2C).

Observation of individual hydration water molecules in protein crystals and in aqueous solution. The NMR experiments in solution described above and x-ray diffraction experiments with protein single crystals are sensitive to different aspects of protein hydration. The intensity of the protein-water NOEs reflects primarily the residence times of the water molecules near the protein protons monitored by the NMR experiment (Fig. 2C). In contrast, the x-ray experiment probes the fraction of time that a water molecule is located at a particular point in space, but is largely insensitive to the residence time at that site on any particular visit (*35*). The main focus of the following discussion is to see how far the x-ray-observations of hydration water in single crystals can be correlated with the residence times of water molecules in corresponding locations observed by NMR in solution.

For oxytocin, where hydration of the entire molecular surface is observable by NMR (Fig. 3), there is no evidence that the sites of the seven and eight water molecules found, respectively, in the two crystal structures of deamino-oxytocin (*4*) are more stably hydrated in solution than the other surface areas. Since oxytocin is flexibly disordered in solution, a more detailed comparison does not seem to be warranted.

BPTI has the same molecular architecture in solution and in

crystals, which includes the four internal water molecules (*14, 36, 37*). In Fig. 5 the crystal structure atomic coordinates (*6*) were used to generate a molecular model visualizing selected surface properties of the protein and the x-ray and NMR observations on surface hydration. The "front view" shown is representative of the complete protein surface. With the possible exception of the protein-protein contact sites in the crystal lattice (yellow in Fig. 5A), the entire protein surface must be covered with hydration water molecules. Only part of the hydration water has so far been observed by either of the two methods considered here. In the BPTI crystal structure, ~40 percent of the protein surface is involved in protein-protein contacts, 25 percent is covered with x-ray–observable hydration water attributed to the central protein molecule, and for an additional 15 percent there are contacts with water molecules attributed to neighboring protein molecules (Fig. 5B). The remaining 20 percent of the protein surface must be in contact with water molecules that are not sufficiently well ordered to be seen by x-ray diffraction (see also Fig. 5A, where white color indicates water-accessible hydrogen atoms). More than 40 percent of the x-ray–observable water molecules are in contact with two protein molecules in the crystal lattice, and all of the observed waters are in contact with one protein molecule. Interestingly, most of the observed surface hydration water molecules are also accessible for contact with x-ray–unobservable water in the crystal. In aqueous solution all polypeptide hydrogen atoms giving rise to negative σ^{NOE} values with the water resonance (brown in Fig. 5C) are located near the amino terminus or a carboxyl or hydroxyl proton (magenta in Fig. 5C) or near one of the four interior water molecules (green in Fig. 5C). On the basis of additional NMR measurements and observations on the locations of the x-ray–observable hydration water molecules in BPTI crystals (see below), we arrive at two important conclusions on surface hydration in solution: (i) Nearly all NOEs with negative σ^{NOE} values between the water resonance and resonances of protons on the

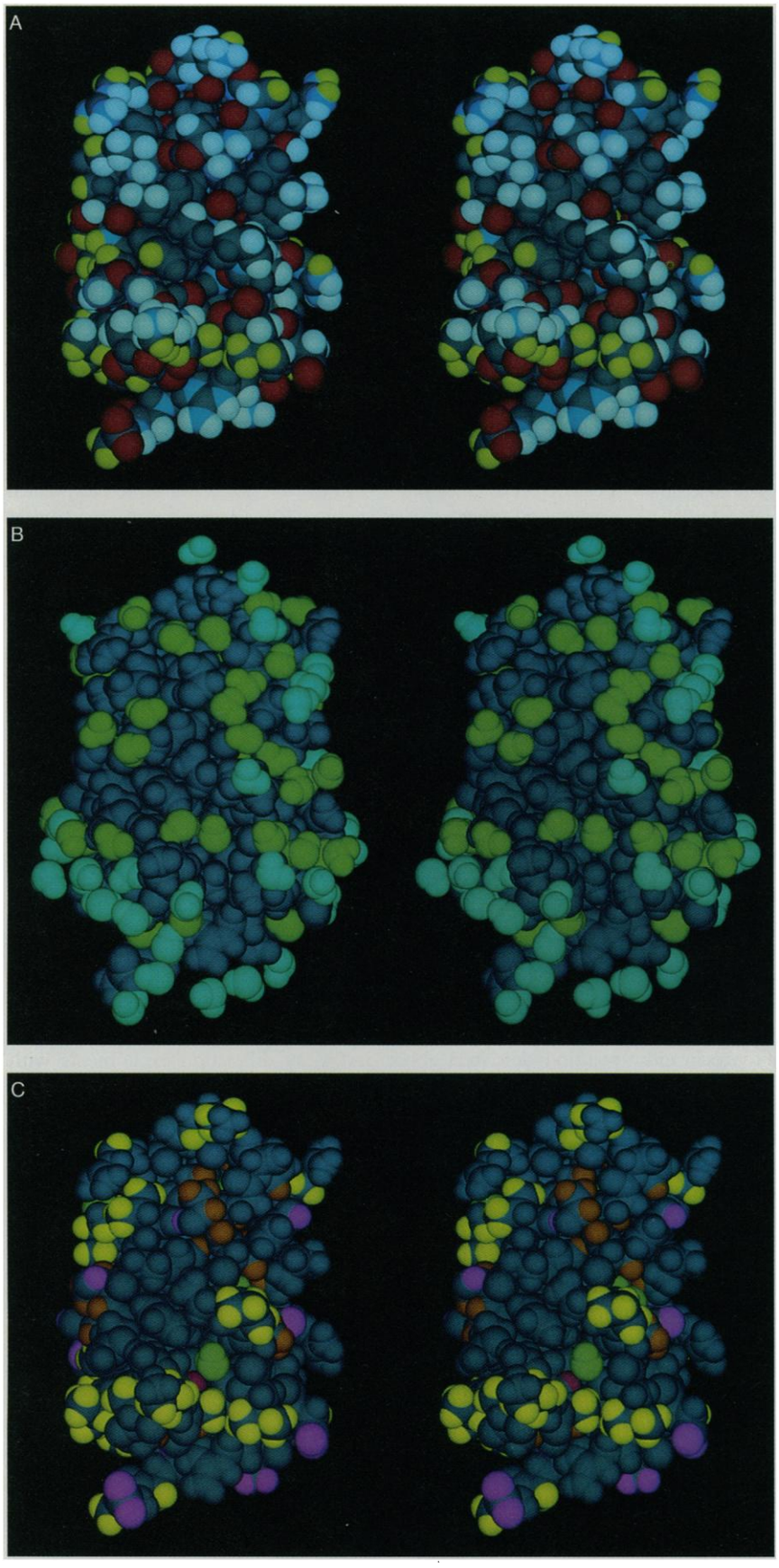

Fig. 5. Stereoviews of a space-filling CPK representation of the crystal structure of BPTI (*6*). The following color codes are used to visualize salient features of the structure in crystals and in solution. (**A**) Protein surface. Hydrogen, carbon, and sulfur atoms, gray; nitrogen, blue; oxygen, red; hydrogen atoms with more than 20 percent solvent-accessible surface area in the single crystal, white; and hydrogen atoms within a distance of ≤ 3.0 Å from neighboring protein molecules in the crystal lattice, yellow. (**B**) Hydration observed in crystals. Polypeptide atoms, gray; water molecules attributed to this protein molecule in the crystal, green; and additional water molecules attributed to hydration sites on neighboring protein molecules yet located within 3.0 Å, blue-green. (**C**) NMR observations in aqueous solution. Hydrogen atoms for which ^{1}H-^{1}H NOE cross peaks with the water resonance were observed, brown (σ^{NOE} negative) or yellow (σ^{NOE} positive); polypeptide atom groups with proton chemical shifts at the water resonance, magenta (exchangeable hydrogens from side-chain hydroxyls and the amino terminus; carboxyl oxygens); interior waters and the surface-bound water molecules W129 and W143 observed identically in all three crystal structures (*5–7*), green; and hydrogen-bonding partner of W143 (Ala^{25} NH), red.

protein surface are due to the hydroxyl protons of Ser, Thr, and Tyr, rather than to stably bound water molecules; and (ii) the surface hydration sites with well-ordered, x-ray–observable water molecules in the crystal structure have similar residence times for bound water in solution as other surface areas for which no hydration water is seen by x-ray diffraction (Fig. 5).

The conclusion (i) is supported by NMR observations made at 4°C in the pH range 5.0 to 6.5, where the chemical exchange of the hydroxyl protons of Ser, Thr, and Tyr becomes sufficiently slow [figure 2.3 in (*11*)] for separate signals to be seen away from the water line. Under these conditions the NOEs between nonlabile polypeptide protons and the hydroxyl proton resonances were observed as strong cross peaks with negative σ^{NOE} values that are well separated from the water chemical shift. These same NOEs are observed in the cross plane of Fig. 4 at the water frequency, since at pH 3.5 the hydroxyl protons exchange more rapidly and their resonances are coalesced with the water signal.

The conclusion (ii) results from two quite independent observations. First, out of a total of approximately 60 x-ray–observable surface hydration waters there are only six water molecules that have conserved hydrogen-bonding partners in all three single-crystal structures of BPTI (*5–7*). Of those, the hydration sites W143 and W129 (Fig. 5C; W, water) could so far be characterized by the NMR data. In the crystal structures, W143 is in hydrogen-bonding distance to the amide proton of Ala^{25}, which has vanishing cross peak intensity with the water line in NOESY and a weak NOE cross peak in the ROESY spectrum. W129 is within hydrogen-bonding distance of the amide proton of Ile^{19}, which interacts with a positive σ^{NOE} rate with the water. From these data, upper limits for the residence times can be established as <500 ps for W143 and <300 ps for W129, that is, the same as for other surface hydration waters. Second, in the crystal structure 5PTI (*6*) more than 50 percent of the x-ray–observable water molecules are within 3.0 Å of a backbone carbonyl oxygen, 40 percent are near a charged group, and only ~10 percent (7 out of a total of 63 water molecules) are in contact with the uncharged -OH groups of the eight residues of Ser, Thr, and Tyr. If the x-ray–observable surface hydration sites were characterized by outstandingly long residence times of the hydration water molecules in solution and correspondingly large negative σ^{NOE} values (Fig. 2C), there would be clear-cut discrepancies with the results of the NMR experiments. These experiments showed strong negative NOEs with the water resonance for protons near the -OH groups of Ser, Thr, and Tyr, which have already been shown to correspond to direct NOEs with these protons. Only a small number of additional NOEs with negative σ^{NOE} values were observed between the water resonance and polypeptide protons located on the protein surface, of which all but one could be assigned to proximity to the NH_2-terminal amino group. There were no strong NOE cross peaks with negative σ^{NOE} values left that could be attributed to the preferred binding sites for ordered hydration water, which are near the carbonyl oxygens and charged groups in the crystal structure. It can therefore be excluded that water molecules in these sites in the solution structure have significantly longer residence times than the other surface hydration waters.

Implications for protein hydration. X-ray data on protein crystals and NMR observation of individual hydration water molecules in solution agree in one aspect of protein hydration: Interior waters, which are part of the protein molecular architecture, are observed in identical locations of the protein molecule in solution and in crystals (*14, 21*). A general structural characterization of hydration sites that give rise to "interiorlike" behavior of the bound water molecules is therefore an interesting project for future research. A crucial difference between the results obtained with the two methods is that although there is a priori no x-ray evidence to distinguish between the properties of the interior waters and highly occupied surface hydration sites, these two types of hydration sites are clearly distinguished by the residence times of the water molecules manifested in the sign of σ^{NOE} in solution. For the interior waters the residence time is in the range of about 10^{-2} to 10^{-8} s (*22*), whereas for surface hydration waters it is in the subnanosecond range even at 4°C. The presently available evidence as described in this article implies that the extent to which the surface hydration water molecules are ordered, and hence observable by x-ray diffraction in protein crystals, cannot be correlated with significantly longer residence times of water molecules in the corresponding sites in solution. The experience gained with the NMR experiments shows that at 4°C, different residence times in the range <500 ps can be found for different individual surface hydration waters (yellow in Fig. 5C). Although a quantification of these differences would at present be premature, future improvements of the sensitivity of the NOE experiments should enable further refinements of the description of protein surface hydration in solution.

With regard to protein structure and function in aqueous milieus the surface hydration water provides a flexible matrix enabling the polypeptide chain to respond efficiently to environmental changes during processes such as protein folding, protein-protein complexation, and enzyme-substrate interaction. The permanent rearrangement of the hydration network on the protein surface must be an important factor for rapid approach to a near-global energy minimum in these processes, which also shows that any intermolecular recognition of a protein surface includes the characteristics of an induced fit [see, for example, (*38*)].

REFERENCES AND NOTES

1. F. M. Richards, *Sci. Am.* **264**, 34 (January 1991).
2. G. E. Schulz and R. H. Schirmer, *Principles of Protein Structure* (Springer-Verlag, New York, 1979).
3. J. D. Glickson, in *Peptides: Chemistry, Structure, Biology*, R. Walter and J. Meienhofer, Eds. (Ann Arbor Science, Ann Arbor, MI, 1975), pp. 787–802; V. J. Hruby, in *Topics in Molecular Pharmacology*, A. S. V. Burgen and G. C. K. Roberts, Eds. (North-Holland, Amsterdam, 1981), pp. 100–125.
4. S. P. Wood *et al.*, *Science* **232**, 633 (1986).
5. J. Deisenhofer and W. Steigemann, *Acta Crystallogr.* **B31**, 238 (1975).
6. A. Wlodawer, J. Walter, R. Huber, L. Sjölin, *J. Mol. Biol.* **180**, 301 (1984).
7. A. Wlodawer, J. Nachman, G. L. Gilliland, W. Gallagher, C. Woodward, *ibid.* **198**, 469 (1987).
8. T. L. Blundell and L. N. Johnson, *Protein Crystallography* (Academic Press, New York, 1976).
9. In one case, crambin, ring structures formed by mutually hydrogen-bonded water molecules on the protein surface were reported: M. M. Teeter, *Proc. Natl. Acad. Sci. U.S.A.* **81**, 6014 (1984).
10. F. C. Bernstein *et al.*, *J. Mol. Biol.* **122**, 535 (1977).
11. K. Wüthrich, *NMR of Proteins and Nucleic Acids* (Wiley, New York, 1986).
12. ———, *Science* **243**, 45 (1989).
13. ———, *Acc. Chem. Res.* **22**, 36 (1989).
14. G. Otting and K. Wüthrich, *J. Am. Chem. Soc.* **111**, 1871 (1989).
15. G. Otting, E. Liepinsh, B. T. Farmer II, K. Wüthrich, *J. Biomol. NMR* **1**, 209 (1991).
16. F. Solomon, *Phys. Rev.* **99**, 559 (1955); A. Abragam, *Principles of Nuclear Magnetism* (Clarendon, Oxford, 1961).
17. R. G. Bryant and W. S. Shirley, *Biophys. J.* **32**, 3 (1980); B. Halle, T. Andersson, S. Forsén, B. Lindman, *J. Am. Chem. Soc.* **103**, 500 (1981); S. H. Koenig, *Biophys. J.* **53**, 91 (1988).
18. C. F. Polnaszek and R. G. Bryant, *J. Chem. Phys.* **81**, 4038 (1984).
19. T. P. Pitner, J. D. Glickson, J. Dadok, G. R. Marshall, *Nature* **250**, 582 (1974); J. D. Glickson *et al.*, *Biochemistry* **15**, 1111 (1976); J. D. Stoesz, A. G. Redfield, D. Malinowski, *FEBS Lett.* **91**, 320 (1978).
20. G. Otting and K. Wüthrich, in *Water and Ions in Biomolecular Systems*, D. Vasilescu, J. Jaz, L. Packer, B. Pullman, Eds. (Birkhäuser, Basel, 1990), pp. 141–147.
21. G. M. Clore, A. Bax, P. T. Wingfield, A. Gronenborn, *Biochemistry* **29**, 567 (1990).
22. G. Otting, E. Liepinsh, K. Wüthrich, *J. Am. Chem. Soc.* **113**, 4363 (1991).
23. B. A. Messerle, G. Wider, G. Otting, C. Weber, K. Wüthrich, *J. Magn. Reson.* **85**, 608 (1989).
24. A. A. Bothner-By, R. L. Stephens, J. Lee, C. D. Warren, R. W. Jeanloz, *J. Am. Chem. Soc.* **106**, 811 (1985).
25. A. Kalk and H. J. C. Berendsen, *J. Magn. Reson.* **24**, 343 (1976).
26. R. Richarz, K. Nagayama, K. Wüthrich, *Biochemistry* **19**, 5189 (1980).

27. T. Fujiwara and K. Nagayama, *J. Chem. Phys.* **83**, 3110 (1985).
28. Y. Ayant, E. Belorizky, P. Fries, J. Rosset, *J. Phys.* (*Paris*) **38**, 325 (1977).
29. K. T. Gillen, D. C. Douglass, M. J. R. Hoch, *J. Chem. Phys.* **57**, 5117 (1972).
30. S. Meiboom, *ibid.* **34**, 375 (1961).
31. In Fig. 3 such exceptions with positive NOESY cross peaks are the amide proton of Tyr^2 and the side-chain amide protons of Gln^4, where the chemical exchange with the water dominates over the NOE in the NOESY spectrum. The broad positive peak at 8.35 ppm is due to chemical exchange of the amino group of Cys^1.
32. The ratio $\sigma^{NOE}/\sigma^{ROE}$ is −0.5 for the intensities of the CαH-NH cross peaks between sequentially neighboring amino acid residues, in agreement with $\tau_R = 2$ ns.
33. Exceptions with significantly different $\sigma^{NOE}/\sigma^{ROE}$ values are the CαH and CβH resonances of Cys^1, which show strong cross peaks with the water signal in the ROESY spectrum (Fig. 3C) but vanishing cross peak intensity in the corresponding NOESY trace (Fig. 3B). This is due to a superposition of NOEs with hydration water and NOEs with the protons of the αNH_3^+ group of Cys^1. Both NOEs have the same sign in ROESY but opposite sign in NOESY. Similar cancellation may be effective in the cross peak between the water signal and the CεH resonance of Tyr^2, where the σ^{NOE} rate with the labile side chain hydroxyl proton of Tyr^2 would be of opposite sign than the σ^{NOE} rate due to the interaction with hydration water.
34. The diagonal in Fig. 4 corresponds to the 1D cross section through the water line in a 2D NMR spectrum as shown in Fig. 3, except that because of the lesser digital resolution of about 0.1 ppm per point in the ω_1 dimension, the water signal in the 3D NMR spectrum is not completely resolved from all α-proton resonances of the protein, that is, the α-proton resonance of Cys^{38} overlaps with the water signal, and therefore its intraresidual NOEs with βCH_2 appear on the diagonal. See also (*15*).
35. W. Saenger, *Annu. Rev. Biophys. Biophys. Chem.* **16**, 93 (1987).
36. G. Wagner *et al.*, *J. Mol. Biol.* **196**, 611 (1987).
37. K. Berndt, P. Güntert, L. Orbons, K. Wüthrich, unpublished results.
38. D. E. Koshland, G. Neméthy, D. Filmer, *Biochemistry* **5**, 365 (1966).
39. Abbreviations for the amino acid residues are: A, Ala; C, Cys; G, Gly; I, Ile; K, Lys; L, Leu; M, Met; N, Asn; P, Pro; Q, Gln; R, Arg; and Y, Tyr.
40. Supported by the Schweizerischer Nationalfonds (project no. 31.25174.88). We thank T. J. Richmond for helpful discussions, Xia Tai-He for help with the solvent accessibility computation using the program ANAREA [T. J. Richmond, *J. Mol. Biol.* **178**, 63 (1984)], and R. Marani for the careful processing of the manuscript.

9 August 1991; accepted 16 October 1991

"What's come over Heisenberg? He seems to be certain about everything *these days."*